Terahertz emission by balanced nonlinear effects in air plasma

Rongjie Xu (许荣杰)[1,2], Ya Bai (白 亚)[2], Liwei Song (宋立伟)[2], Na Li (李 娜)[2], Peng Peng (彭 鹏)[2], and Peng Liu (刘 鹏)[1,2*]

[1] *MOE Key Laboratory of Advanced Micro-structured Materials, Institute of Precision Optical Engineering, School of Physics Science and Engineering, Tongji University, Shanghai 200092, China*

[2] *Shanghai Institute of Optics and Fine Mechanics, Chinese Academy of Sciences, Shanghai 201800, China*

[*] *Corresponding author: peng@siom.ac.cn*

Received September 17, 2013; accepted November 5, 2013; posted online December 9, 2013

The evolution of terahertz (THz) waveform in air plasma driven by low-energy few-cycle laser pulses is investigated to improve the accuracy of the carrier envelope phase (CEP) determination. Based on the transient photocurrent model, a balanced spatial distribution of the Kerr and free-electron effects in the plasma is found at 109 μJ input energy. THz inversion occurs only once at the initial CEP of 0.5π, in which high-precision measurement of the CEP of few-cycle laser pulses is achieved.

OCIS codes: 300.6495, 140.7090, 260.3060, 350.5400.
doi: 10.3788/COL201311.123002.

Air filament driven by strong femtosecond (fs) laser pulses has various important applications, which include remote sensing, controlling the weather, and spectral broadening of ultra-short pulse generation[1−10]. For an ultra-short laser pulse that contains only a few cycles of carrier wave, its carrier envelope phase (CEP) is a significant parameter in modifying the laser field and the outcomes of interaction with a medium[11−13]. Air filament driven by few-cycle laser pulses can emit broadband radiation with spectrum that extends to the terahertz (THz) region[14]. The transient photocurrent model indicates that the enhanced THz radiation is produced by the asymmetric photocurrents induced by the accelerated photoelectrons, which is modulated as a function of CEP[15]. Therefore, THz spectroscopy can be used as a convenient method for measuring CEP, rather than the state-of-the-art stereo above threshold ionization (ATI) measurement[16,17].

In a filament driven by focusing few-cycle laser fields, the nonlinear effects of plasma and Kerr focusing lead to a modified Gouy shift, which vary depending on the input pulse energy[18]. Such phase-shift variation in plasma hinders the accurate determination of the CEP value, so the initial CEP is proposed to characterize the phase of few-cycle laser pulses[19]. Given the dependence of THz emission on CEP, inversion of THz waveforms along the plasma can probe the accurate CEP value. In this scheme, the inversion position of THz emission from negative to positive polarity moves to the start of the filament and disappears when the initial CEP increases to 0.5π, thereby providing a flag of the CEP value. The proposed method and experimental confirmation are performed with moderate (400 μJ) energy driving laser pulse, one or two inversions of THz emission in air plasma, and the accuracy of the determined CEP value is limited to 73 mrad. The error results from the little CEP shift of the propagating few-cycle pulses because of the distortion of the pulse envelope by the nonlinear effects in plasma. At low-input energy (<250 μJ) driving pulses, the accuracy of CEP is expected to increase because of less pulse-front distortion. However, the characteristics of THz modulation in air plasma by low-energy few-cycle pulses are still unknown. In addition, the interacting nonlinear effects in plasma need further investigation for a more accurate determination of the initial CEP value of few-cycle pulses.

In this letter, we report the propagation of a focusing few-cycle laser pulse in ionizing air plasma and the corresponding THz emission using driving pulse energy from 20 to 200 μJ. Within this energy region, the plasma effect on the pulse envelope function decreases to a magnitude that is comparable with the diffraction and Kerr effects, and a balanced phase-variation canceling is found near 109 μJ. The polarity of the resulting THz waveforms is reversed only when the initial CEP is 0.5π with an error of 50 mrad, thereby revealing improved accuracy of the initial CEP determination. Moreover, the flattening of CEP variation suggests THz enhancement produced by few-cycle pulses.

We apply the photocurrent model to calculate the THz radiation driven by propagating few-cycle pulses in air plasma[20,21]. The intense few-cycle laser fields in a dispersive medium can be described by the propagation equation in Ref. [22] in axial-symmetric coordinates,

$$\partial_z \widetilde{E}(r,z,\omega) = \Big[\frac{\mathrm{i}}{2k(\omega)}\nabla_\perp^2 + \mathrm{i}k(\omega)\Big]\widetilde{E}(r,z,\omega) + \frac{\mathrm{i}\omega^2}{2c^2\varepsilon_0 k(\omega)}\widetilde{P}_{\mathrm{NL}} + \frac{\omega}{2c^2\varepsilon_0 k(\omega)}\widetilde{J}_{\mathrm{ioni}}, \quad (1)$$

where $\widetilde{E}(r,z,\omega)$ is the Fourier-transform of the time-domain laser field $E(r,z,t)$. The first term on the right-hand side of Eq. (1) describes the linear dispersion and diffraction of the pulse. The nonlinear polarization $\widetilde{P}_{\mathrm{NL}}$ originates from the optical Kerr effect. The ionization current $\widetilde{J}_{\mathrm{ioni}}$ generated from the tunneling ionization of N_2 and O_2 in air accounts for the plasma effect. Optical intensity can be obtained by $|E(r,z,t)|^2$. The tunnel-

ing ionization rate of gas molecules (Ammosov-Delone-Krainov model) can be written as[15,23]

$$W_{\mathrm{ADK}}(t) = \frac{\alpha}{[E(t)/E_{\mathrm{a}}]^{2n-1}} \exp\Big[-\frac{\beta}{E(t)/E_{\mathrm{a}}}\Big], \quad (2)$$

where $\alpha = \omega_{\mathrm{ion}}|C_n|^2(2r_{\mathrm{H}}^{3/2})^{2n-1}$, $\beta = \frac{2}{3}r_{\mathrm{H}}^{3/2}$, $\omega_{\mathrm{ion}} = U_{\mathrm{ion}}/\hbar$, $n = r_{\mathrm{H}}^{-1/2}$, $r_{\mathrm{H}} = U_{\mathrm{ion}}/U_{\mathrm{H}}$ is the ionization potential of the gas molecules under consideration relative to that of hydrogen ($U_{\mathrm{H}} \approx 13.6$ eV), $|C_n|^2 = 2^{2n}\{n\Gamma(n)\Gamma(n+1)\}^{-1}$, $E_{\mathrm{a}} = m^2e^5/(4\pi\varepsilon_0)^3\hbar^4 \approx 5.14 \times 10^{11}$ Vm^{-1}, and $E(t)/E_{\mathrm{a}}$ is the electric field in atomic units. The generated plasma density $\rho_{\mathrm{e}}(t)$ can be written as

$$\frac{\partial\rho_{\mathrm{e}}(t)}{\partial t} = W_{\mathrm{ADK}}(t)[\rho_{\mathrm{at}} - \rho_{\mathrm{e}}(t)], \quad (3)$$

where ρ_{at} is the neutral atomic density. The collective motion of the tunneling ionized electrons results in a directional nonlinear photocurrent surge described in Ref. [24]:

$$\partial_t J_{\mathrm{e}}(r,z,t) + \nu_{\mathrm{e}} J_{\mathrm{e}}(r,z,t) = \frac{e^2}{m}\rho_{\mathrm{e}}(r,z,t)E(r,z,t), \quad (4)$$

where ν_{e}, e, m, and ρ_{e} denote the electron–ion collision rate, electron charge, mass, and electron density, respectively. The transient current at each propagation step of the calculation is treated as radiation source of far-field THz emission[25],

$$E_{\mathrm{THz}}(r',t) = -\frac{1}{4\pi\varepsilon_0}\int \frac{1}{c^2R}\partial_t J_{\mathrm{e}}(r,z,t_r)\mathrm{d}^3r. \quad (5)$$

In our calculations, we used a Gaussian beam as initial driving laser field with waist size of $\omega_0 = 180$ μm ($1/e^2$) at 1.8-μm wavelength and 11-fs duration (~ 1.8 optical cycles) in full width at half maximum (FWHM).

Using Eq. (5), the calculated THz amplitude ($|E_{\mathrm{THz}}|$) versus filament length and initial CEP were obtained (Figs. 1(a) to (c)) at input energies of 20, 109, and 200 μJ, respectively. The position of $z = 0$ is set to be the linear focusing position for the convenience of calculation. Figures 1(d) and (f) show the positions of THz inversion retrieved for all of the initial CEP values in a step size of 0.1π. At low input energy (20 μJ), the number of inversions of THz waveforms along the filament is one or none for all of the CEP values. For the initial CEP of 0 to 1.0π, the positions of inversion move downstream of the filament, and the slope of the THz inversion position is positive. When the energy of the laser pulses is increased to 109 μJ (Fig. 1(b)), the THz amplitude remains zero along the plasma with initial CEP value near $\varphi_0 = 0.5\pi$. For the initial CEP value other than $\varphi_0 = 0.5\pi$, the THz amplitude increases monotonically in the filament. As indicated in Fig. 2, THz emission for $\varphi_0 = 0.4\pi$ and 0.6π remains negative or positive with little modulation. This phenomenon is due to the fact that the variation in the CEP in plasma is not significant enough (flattened appearance) to change its polarity in the vicinity of focus (Fig. 3). Given the distortion of pulse front in the beginning of the filament[19], the THz amplitude of $\varphi_0 = 0.5\pi$ at the beginning of the filament is near zero and easily affected by the CEP variation, thereby leading to the subsequent inversion of polarity of THz emission. Therefore, only a weaker THz emission from the initial CEP of $\varphi_0 = 0.5\pi$ may result in the inversion of THz polarity. Increasing the energy of laser pulses to 200 μJ also increases the number of THz inversions. For the initial CEP of 0 to 0.5π, the inversion positions of THz waveform gradually shift to the beginning of the filament, and the slope of the THz inversion position is negative.

For comparison, we calculate the THz amplitude at different filament lengths and initial CEP values under linear focusing without propagation effect. At different input energies, for the initial CEP of 0 to 1.0π, the position of inversion moves downstream of the filament, and the slope of the THz inversion position is always

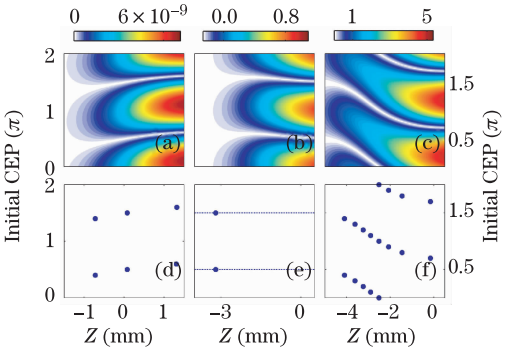

Fig. 1. Calculated THz amplitude ($|E_{\mathrm{THz}}|$) as a function of plasma length at initial CEP of 1.8-cycle laser pulses with input energies of (a) 20, (b) 109, and (c) 200 μJ. The retrieved inversion positions of THz emission at (d) 20, (e) 109, and (f) 200 μJ. z is the propagation coordinate.

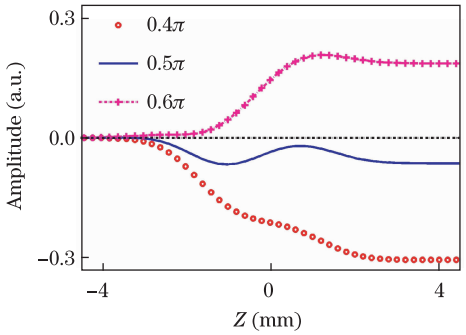

Fig. 2. Calculated THz amplitude as a function of filament length for the initial CEP of φ_0 =0.4π, 0.5π, 0.6π, at 109 μJ input energy.

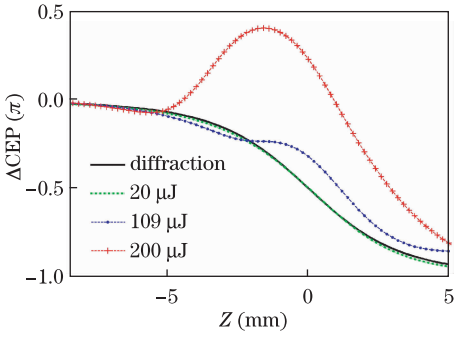

Fig. 3. Variation in CEP along the air plasma at different input energies.

positive, similar to the results shown in Figs. 1(a) and (d). The propagation effect at a low input energy (20 μJ) is considerably small such that the CEP variations have nonsignificant variations compared with that under linear focusing condition (Fig. 3).

A demarcation emerges between the positive and negative slopes of the THz inversion position as energy increases. The CEP of the driving few-cycle fields varies along the filament because of the nonlinear propagation effects, which include Kerr and plasma effects as well as the modified Gouy phase shift. CEP variation also changes with increasing pulse energy, thereby resulting in variations in THz inversion.

Within the air plasma, the refractive index changes because of the following effects: the Kerr self-focusing effect, which is defined as $\Delta n_{\rm kerr} = n_2 I$, where n_2 is the air nonlinear index of refraction, and I is the intensity; the formation of plasma, which is defined as $\Delta n_{\rm plasma} = -N_{\rm e}e^2/2\varepsilon_0 m_{\rm e}\omega_0^2$, where $N_{\rm e}$ corresponds to the plasma density, e is the electron charge, $m_{\rm e}$ is the mass of the electron, ε_0 is the vacuum permittivity, and ω_0 is the pulse's central angular frequency[26,27]. As shown in Fig. 3, at low input energy (20 μJ), the CEP variation, similar to that of pure diffraction effect, decreases smoothly because of the least propagation effect. The slope of CEP variation is constantly negative, which corresponds to the positive derivative of THz inversion position. At increased energy of laser pulses (109 μJ), Kerr effect decreases CEP further at the front of the filament. Our calculation indicates that $\Delta n_{\rm kerr} = -\Delta n_{\rm plasma} = 5.8 \times 10^{-5}$ at $z = -2.4$ mm. Given the increasing electron density, the plasma effect participates and counteracts with the Kerr self-focusing effect. The sum of the plasma and Kerr effects decelerates the decrease in CEP, which tends to be level near the focus ($z = -2.4$ to –1.2 mm). The CEP increment near the focus becomes smaller, thereby producing less inversion number of THz emission. With an additional increase in energy of laser pulses (200 μJ), in the middle and end parts of the filament, the CEP variations show significant increase and decrease (hump structure), which result in the variation in THz inversion. In addition, the CEP increment becomes larger. Compared with the result at energy $<$ 109 μJ, the slope of CEP variation shows a hump structure, thereby resulting in the negative slope of the THz inversion position.

The intensity within the filament is an important parameter in describing a filamentation process[28]. The competition between Kerr and plasma effects leads to a clamping of the peak intensity[29], which represents the dynamic balance of the nonlinear effects in air plasma. The calculated peak intensity (blue solid line) and peak electron densities (red dotted dashed line) at different pulse energies in the air filament caused by the laser with a central wavelength of 1.8 μm are shown in Fig. 4. The turning points are at approximately 101 μJ in the peak intensity curve and at approximately 131 μJ in the electron density curve, which are obtained by drawing two tangential straight lines through the increasing and flattened parts of the two curves. When the input energy is $<$ 101 μJ, a steep increase in the peak intensity in the filament is observed as the input pulse energy increases. In such case, Kerr effect is dominant in causing a

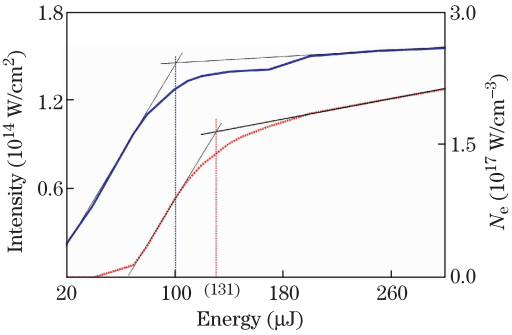

Fig. 4. (Color online) Calculated peak intensity (blue solid line) and peak electron densities (red dashed line) at the different pulse energies in air filament.

variation in the laser field. When the energy is $>$ 101 μJ, the increasing electron densities increase the plasma effect, thereby counteracting the Kerr self-focusing effect. The 109 μJ energy, which is between 101 and 131 μJ, is the energy at which the CEP variation becomes smaller and tends to be leveled near the focus of the filament because the plasma effect starts to be comparable with Kerr effect (Fig. 3). Hence, only one inversion of THz waveform for the CEP of 0.5π and the optimal accuracy of CEP determination are obtained at 109 μJ. This unique feature in THz emission can also indicate the initiation of the balance between the plasma and Kerr effects. The difference in energies may be have been caused by the extra energy needed to accelerate the tunneling ionized electrons to generate transient photocurrents.

In conclusion, we investigate the spatial distribution of the nonlinear effects and THz emission in air plasma driven by intense few-cycle laser fields at relatively low energy ($<$ 200 μJ). The calculations based on the transient photocurrent model indicate that THz inversion occurs only once at initial CEP of 0.5π because of the Kerr and free-electron effects on the driving pulses. With improved THz detection sensitivity, the experimental results are measured. The proposed measurement provides a method to enhance the accuracy of measuring the CEP of few-cycle laser pulses.

This work was supported by the Chinese Academy of Sciences, the Chinese Ministry of Science and Technology, the National Natural Science Foundation of China (Nos. 60978012, 11274326, 11134010, and 11127901), and the National "973" Program of China (No. 2011CB808103).

References

1. W. Liu, F. Théberge, J.-F. Daigle, P. T. Simard, S. M. Sarifi, Y. Kamali, H. L. Xu, and S. L. Chin, Appl. Phys. B **85,** 55 (2006).
2. T. Wang, S. Yuan, Y. Chen, and S. Chin, Chin. Opt. Lett. **11,** 011401 (2013).
3. P. Rohwetter, J. Kasparian, K. Stelmaszczyk, Z. Q. Hao, S. Henin, N. Lascoux, W. M. Nakaema, Y. Petit, M. Quießer, R. Salamé, E. Salmon, L. Wöste, and J. P. Wolf, Nat. Photon. **4,** 451 (2010).
4. J. Ju, J. Liu, C. Wang, H. Sun, W. Wang, X. Ge, C. Li, S. L. Chin, R. Li, and Z. Xu, Opt. Lett. **37,** 1214 (2012).

5. J. Ju, J. Liu, C. Wang, H. Sun, W. Wang, X. Ge, C. Li, S. L. Chin, R. Li, and Z. Xu, Appl. Phys. B **110,** 375 (2013).
6. J. Kasparian, M. Rodriguez, G. Méjean, J. Yu, E. Salmon, H. Wille, R. Bourayou, S. Frey, Y.-B. André, A. Mysyrowicz, R. Sauerbrey, J. P. Wolf, and L. Wöste, Science **301,** 61 (2003).
7. V. P. Kandidov, O. G. Kosareva, I. S. Golubtsov, W. Liu, A. Becker, N. Akozbek, C. M. Bowden, and S. L. Chin, Appl. Phys. B **77,** 149 (2003).
8. F. Théberge, W. Liu, Q. Luo, and S. L. Chin, Appl. Phys. B **80,** 221 (2005).
9. J. Kasparian and J. P. Wolf, Opt. Express **16,** 466 (2008).
10. S. L. Chin, S. A. Hosseini, W. Liu, Q. Luo, F. Théberge, N. Aközbek, A. Becker, V. P. Kandidov, O. G. Kosareva, and H. Schroeder, Can. J. Phys. **83,** 863 (2005).
11. A. Baltuska, Th. Udem, M. Uiberacker, M. Hentschel,E. Goulielmakis, Ch. Gohle, R. Holzwarth, V. S.Yakovlev, A. Scrinzi, T. W. Hansch, and F. Krausz, Nature **421,** 611 (2003).
12. A. Apolonski, P. Dombi, G. G. Paulus, M. Kakehata, R.Holzwarth, Th. Udem, Ch. Lemell, K. Torizuka, J.Burgdörfer, T. W. Hänsch, and F. Krausz, Phys. Rev. Lett. **92,** 073902 (2004).
13. T. Nakajima and S. Watanabe, Phys. Rev. Lett. **96,** 213001 (2006).
14. W. Wang, Z. Sheng, Y. Li, L. Chen, Q. Dong, X. Lu, J. Ma, and J. Zhang, Chin. Opt. Lett. **9,** 110002 (2011).
15. H. G. Roskos, M. D. Thomson, M. Kreß, and T. L. Löffler, Laser Photon. Rev. **1,** 349 (2007).
16. M. Kreß, T. Löffler, M. D. Thomson, R. Dörner, H. Gimpel, K. Zrost, T. Ergler, R. Moshammer, U. Morgner, J. Ullrich, and H. G. Roskos, Nat. Phys. **2,** 327 (2006).
17. G. G. Paulus, F. Lindner, H. Walther, A. Baltuška, E. Goulielmakis, M. Lezius, and F. Krausz, Phys. Rev. Lett. **91,** 253004 (2003).
18. Y. Bai, L. Song, R. Xu, C. Li, P. Liu, Z. Zeng, Z. Zhang, H. Lu, R. Li, and Z. Xu, Phys. Rev. Lett. **108,** 255004 (2012).
19. R. Xu, Y. Bai, L. Song, P. Liu, R. Li, and Z. Xu, Appl. Phys. Lett. **103,** 061111 (2013).
20. K. Y. Kim, J. H. Glownia, A. J. Taylor, and G. Rodriguez, Opt. Express **15,** 4577 (2007).
21. K. Y. Kim, A. J. Taylor, J. H. Glownia, and G. Rodriguez, Nat. Photon. **2,** 605 (2008).
22. J. S. Liu, R. X. Li, and Z. Z. Xu, Phys. Rev. A **74,** 043801 (2006).
23. P. B. Corkum, Phys. Rev. Lett. **71,** 1994 (1993).
24. I. Babushkin, W. Kuehn, C. Köhler, S. Skupin, L. Bergé, K. Reimann, M. Woerner, J. Herrmann, and T. Elsaesser, Phys. Rev. Lett. **105,** 053903 (2010).
25. C. Köhler, E. Cabrera-Granado, I. Babushkin, L. Bergé, J. Herrmann, and S. Skupin, Opt. Lett. **36,** 3166 (2011).
26. S. L. Chin, W. Liu, O. G. Kosareva, and V. P. Kandidov, "The Physics of Intense Femtosecond Laser Filamentation", in *Self Focusing*: *Past and Present*, R. W. Boyd, S. G. Lukishova, Y. R. Shen, (eds.) (Springer, New York, 2009).
27. J.-F. Daigle, A. Jaron-Becker, S. Hosseini, T.-J. Wang, Y. Kamali, G. Roy, A. Becker, and S. L. Chin, Phys. Rev. A **82,** 023405 (2010).
28. S. Xu, X. Sun, B. Zeng, W. Chu, J. Zhao, W. Liu, Y. Cheng, Z. Xu, and S. L. Chin, Opt. Express **20,** 299 (2011).
29. A. Couairon and A. Mysyrowicz, Phys. Rep. **441,** 47 (2007).